Macroecological relationships in the dynamics of gut microbiota

Brian W. Ji[1,3], Ravi U. Sheth[1,3], Purushottam D. Dixit[1] & Dennis Vitkup[1,2*]

[1]Department of Systems Biology, Columbia University, New York, NY, USA. [2]Department of Biomedical Informatics, Columbia University, New York, NY, USA. [3]These authors contributed equally. [*]Email: dv2121@cumc.columbia.edu

The gut microbiome is now widely recognized as a dynamic ecosystem that plays an important role in health and disease[1]. While current sequencing technologies make it possible to estimate relative abundances of host-associated bacteria over time[2,3], the biological processes governing their dynamics remain poorly understood. Therefore, as in other ecological systems[4,5], it is important to identify quantitative relationships describing global aspects of gut microbiota dynamics. Here we use multiple high-resolution time series data obtained from humans and mice[6–8] to demonstrate that despite their inherent complexity, gut microbiota dynamics can be characterized by several robust scaling relationships. Remarkably, these patterns are highly similar to those previously observed across diverse ecological communities and economic systems, including the temporal fluctuations of animal and plant populations[9–12] and the performance of publicly traded companies[13]. Specifically, we find power law relationships describing short- and long-term changes in gut microbiota abundances, species residence and return times, and the connection between the mean and variance of species abundances. The observed scaling relationships are altered in mice receiving different diets and affected by context-specific perturbations in humans. We use these macroecological relationships to reveal specific bacterial taxa whose dynamics are significantly affected by dietary and environmental changes. Overall, our results suggest that a quantitative macroecological framework will be important for characterizing and understanding complex dynamical processes in the gut microbiome.

The dynamics of gut bacteria can now be monitored with high temporal resolution using metagenomic sequencing[14]. Recent longitudinal studies have revealed significant day to day variability yet marked long-term stability of gut microbiota[6,7,15,16]. Several studies have also identified important factors, such as host diet and lifestyle, that contribute to temporal changes in species abundances[7,8,17,18]. However, in contrast to macroscopic ecological communities, quantitative relationships describing gut microbiota dynamics are currently not well understood. While ideas from theoretical ecology have been applied to understand static patterns of gut microbial diversity and species abundance distributions[19,20], a comprehensive and quantitative understanding of gut microbiota dynamics is currently missing. Therefore, using a macroecological approach, we sought to investigate dynamical relationships in the gut microbiome using several of the longest and most densely-sampled longitudinal studies in humans and mice[6–8]. The considered data spanned three independent investigations, utilizing different sample collection procedures and sequencing protocols; bacterial abundances in these studies were tracked daily for several weeks in mice and up to a year in humans. Our analysis included four healthy human individuals (A, B, M3, F4) and six individually-housed mice fed either a low-fat, plant polysaccharide (LFPP) diet or a high-fat, high-sugar (HFHS) diet. We use these data to explore the short-term abundance changes and long-term drift of gut microbiota, species residence and return times, and the temporal variability of individual bacterial taxa across humans and different mouse diet groups. Collectively, our study provides the most in-depth and comprehensive characterization of macroecological dynamics in the gut microbiome.

Following a quantitative framework used previously to examine the ecological dynamics of animal populations[9,10], we first investigated short-term temporal fluctuations of gut microbiota abundances. One of the most basic descriptors of bacterial population dynamics is the daily growth rate, defined as the

logarithm of the ratio of consecutive daily abundances, $\mu_k(t) = \log\left(X_k(t+1)/X_k(t)\right)$, where X_k is the relative abundance of a bacterial operational taxonomic unit (OTU) k at time t. Interestingly, we found that the probability of μ averaged over all OTUs closely followed a Laplace distribution, with a characteristic tent shape in log-transformed probabilities (Fig. 1a-c). Laplace distributions were highly similar within and between individual humans, and between humans and mice (parameter $b = 0.73 \pm 0.07$, $b = 0.82 \pm 0.1$; mean $\pm$ s.d. across all humans and LFPP mice respectively), indicating the universality of these relationships. Moreover, the Laplace distribution described well the daily growth rates of every gut microbiome time series we analyzed, including those defined at various taxonomic resolutions (Supplementary Fig. 1). In contrast to a Gaussian growth rate distribution, which is expected for bacterial growth affected by random multiplicative processes[19,21], the Laplace distribution indicates substantially higher probabilities for large short-term bacterial abundance fluctuations. Interestingly, very similar growth rate distributions have been observed across many diverse ecological and economic systems including bird communities[9,10], fish populations[11], tropical rain forests[12], publicly traded company sales[13], and country GDPs[22] (Supplementary Fig. 2a). Similar to these complex ecological and interacting systems, the gut microbiome may exhibit sudden large-scale abundance fluctuations.

In complex ecosystems, species growth rate distributions often depend on their current abundance[10,13,22]. We therefore investigated the relationship between the standard deviation of daily bacterial growth rates and abundances. This analysis revealed that the daily growth rate variability of gut bacteria decreased approximately linearly with increasing mean daily abundances (Fig. 1d-f). Moreover, the observed behavior was similar between human and mouse gut microbiomes (regression slopes $r = -0.15 \pm 0.01$, -0.17 ± 0.03; mean $\pm$ s.d. across humans and mice). Thus, likely due to the presence of more stable nutrient niches, highly abundant bacteria exhibit substantially smaller relative day to day fluctuations compared to bacteria with lower abundances.
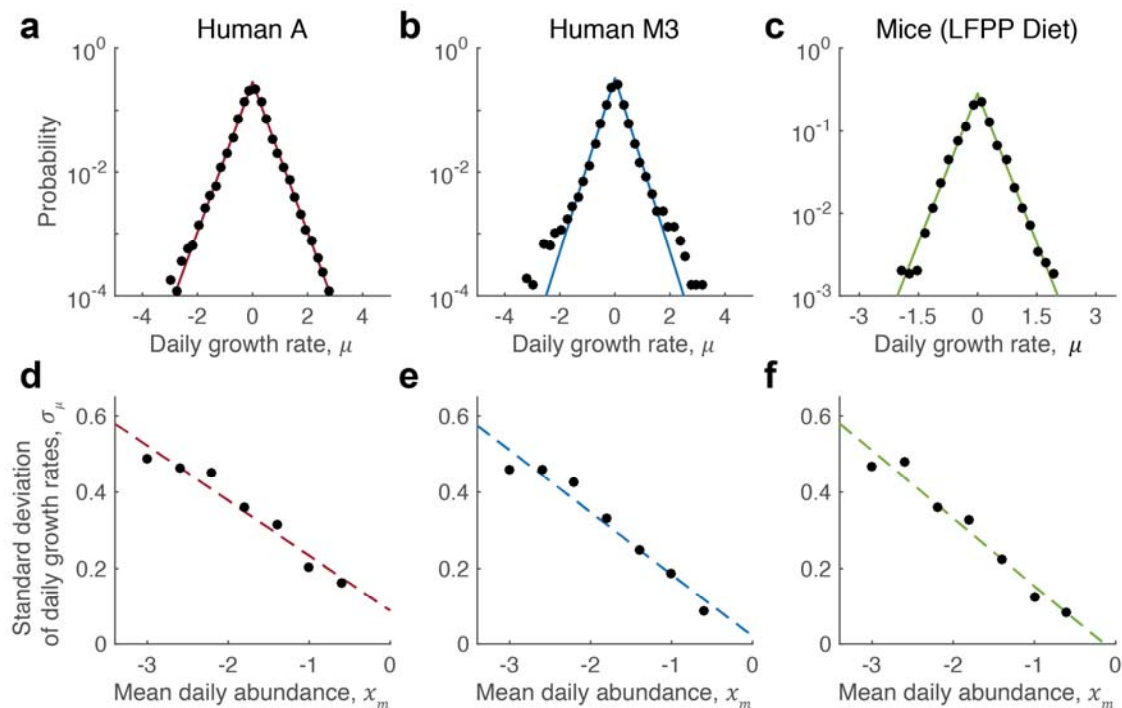

Fig. 1 | Daily changes in the abundances of gut microbiota. a-c, Daily growth rates were defined as $\mu_k(t) = \log\left(X_k(t+1)/X_k(t)\right)$, where X_k is the relative abundance of a given OTU k on day t. The distribution of μ averaged over all OTUs displays a Laplace form, $p(\mu) = \frac{1}{2b}\exp\left(-\frac{|\mu|}{b}\right)$, appearing as a characteristic tent shape in log-

transformed probabilities. Results are shown for two individuals from different human studies (A and M3) and mice fed a low-fat plant polysaccharide-based (LFPP) diet . Laplace exponents are $b = 0.83 \pm 0.1$ for human A, $b = 0.71 \pm 0.07$ for human M3, and $b = 0.82 \pm 0.10$ for LFPP mice (mean $\pm$ s.d., Methods). Solid lines indicate fits to the data using maximum likelihood estimation (MLE). **d-f,** Across all OTUs, the standard deviation of daily growth rates (σ_μ) decreases with mean daily abundance (x_m), defined as the mean of successive log abundances, $x_m = \frac{1}{2}[\log(X(t + 1)) + \log(X(t))]$. Standard deviations were calculated by binning daily growth rates by different values of x_m along the x-axis. Dashed lines are least-squares fits to the data, with slopes of $r = -0.16 \pm 0.02, -0.16 \pm 0.02$ and -0.17 ± 0.03 for A, M3 and LFPP mice respectively (mean $\pm$ s.d., Methods) Growth rates in (**c**) and (**f**) were aggregated across the three mice on the LFPP diet.

In addition to species growth rates, interesting long-term dynamical trends have also been observed across different macroscopic ecosystems[9,23,24]. To explore the long-term behavior of gut microbiota, we investigated how the mean-squared displacement (MSD) of OTU abundances ($\langle \delta^2(\Delta t) \rangle$) changed with time. Again, similar to the behavior of other diverse communities (Supplementary Fig. 2c), we found that the long-term dynamics of gut microbiota abundances could be well approximated by the equation of anomalous diffusion (Fig. 2, Supplementary Fig. 3),

$$\langle \delta^2(\Delta t) \rangle \propto \Delta t^{2H} \quad \#(1)$$

where H is the scaling parameter characterizing the diffusion process, and often referred to as the Hurst exponent[25]. In contrast to normal diffusion ($H = 0.5$), a Hurst exponent of $H > 0.5$ indicates a tendency for increases (decreases) in abundances to be followed by further increases (decreases), whereas a value of $H < 0.5$ indicates a higher degree of stability and a tendency for abundances to revert back to their means. Both in human and mouse gut microbiomes, our analysis revealed small Hurst exponents ($H = 0.09 \pm 0.03$, $H = 0.08 \pm 0.02$, mean $\pm$ s.d. across humans and mice). This suggests that despite overall stability[15,26,27], gut microbiota exhibit a slow, continuous and predictable drift in abundances over long time periods. Furthermore, while the temporal behavior of individual OTU abundances was also well-approximated by the equation of anomalous diffusion (Supplementary Fig. 4a), the distribution of Hurst exponents across individual OTUs exhibited substantial variability (Supplementary Fig. 4b). This demonstrates the heterogeneity in the stability of different gut bacterial taxa within and across hosts. We show below that the stability of different taxa can be significantly affected by environmental factors such as host dietary intake.
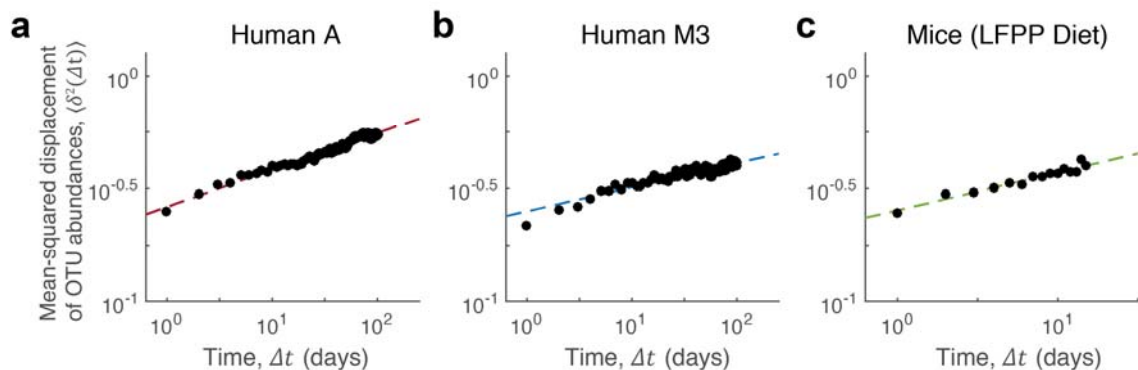

Fig. 2 | Long-term stability of gut microbiota abundances. a-c, In humans and mice, the mean-squared displacement of log OTU abundances ($\langle \delta^2(\Delta t) \rangle$) scales with time as a power law of the form $\langle \delta^2(\Delta t) \rangle \propto \Delta t^{2H}$. Hurst exponents are $H = 0.07 \pm 0.03, 0.08 \pm 0.02, 0.08 \pm 0.02$ for human A, human M3 and LFPP mice respectively (mean $\pm$ s.d.,

Methods). The data in (**c**) represent an average over the three individual mice on the LFPP diet (Methods). Dashed lines indicate least-squares fits to the data.

Both short and long-term dynamics of gut microbiota contribute to overall turnover in gut bacterial species. To directly investigate the dynamics of gut microbiota composition, we next calculated the distribution of residence (t_{res}) and return times (t_{ret}) for individual OTUs. Following previous macroecological analyses[9,28,29], we defined residence times as time intervals between the emergence and subsequent disappearance of corresponding OTUs; analogously, return times were defined as the intervals between disappearance and reemergence of OTUs. Again, we observed patterns very similar to those previously described in diverse ecological communities[9,28,29] (Supplementary Fig. 2b). Specifically, the distributions of t_{res} and t_{ret} followed power laws, with exponential tails resulting from the finite length of the analyzed time series (Fig. 3, Supplementary Fig. 5a,b). Notably, the distributions were also similar within and between individual human and mouse gut microbiomes ($\alpha_{res} = 2.3 \pm 0.05$, $\alpha_{ret} = 1.2 \pm 0.02$, mean $\pm$ s.d. across humans, $\alpha_{res} = 2.2 \pm 0.04$, $\alpha_{ret} = 0.72 \pm 0.03$, across mice on the LFPP diet), suggesting that the processes governing the local emergence and disappearance of gut bacteria are likely to be independent of the specific host.
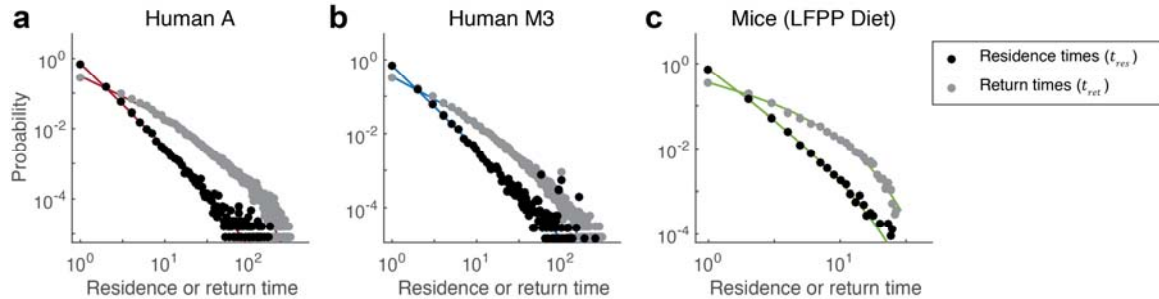

Fig. 3 | Residence and return times of gut microbiota. a-c, Residence (t_{res}) and return times (t_{ret}) were defined as the number of consecutive time points during which an OTU was detected at any abundance in the community or absent from the community respectively. Probability distributions for t_{res} and t_{ret} follow power laws with exponential cutoffs of the form $p(t) \propto t^{-\alpha}e^{-\lambda t}$, with the exponential tail resulting from the finite length of each time series. Power law exponents are $\alpha_{res} = 2.3 \pm 0.04$, 2.2 ± 0.07, 2.2 ± 0.04 for residence times and $\alpha_{ret} = 1.1 \pm 0.02$, 1.2 ± 0.05, 1.2 ± 0.07, 1 for return times (mean $\pm$ s.d., humans A and M3 and LFPP mice respectively, Methods). Residence and return times are aggregated across the three individual mice on the LFPP diet. Solid lines indicate fits to the data using MLE.

Having characterized bacterial growth distributions and residence times, we next investigated the temporal variability of individual OTU abundances. One of the most general relationships in ecology that has been observed across hundreds of different biological communities is known as Taylor's power law[30–32], which connects a species' average abundance to its temporal or spatial variance,

$$\sigma_X^2 = C * \langle X \rangle^\beta \quad \#(2)$$

where C is a constant, $\langle X \rangle$ and σ_X^2 are the mean and variance of species abundances respectively, and β is a positive scaling exponent. For processes following simple Poissonian fluctuations, the parameter $\beta = 1$ and for processes with constant per capita growth variability, $\beta = 2$. Values of β have been empirically observed to lie between 1 and 2 for the vast majority of investigated plant and animal species[33], suggesting that complex ecological interactions may contribute to the observed species dynamics[34]. Our analysis revealed that the temporal variability of gut microbiota also followed Taylor's law (Fig. 4, Supplementary Fig. 6a,b), with exponents for human and mouse gut microbiomes generally consistent with values

observed previously in other ecological communities[33] ($\beta = 1.7 \pm 0.02$ across humans, $\beta = 1.49 \pm 0.02$ across LFPP mice). Notably, dynamics consistent with Taylor's law have also been observed in a recent short-term analysis of the healthy human vaginal microbiome[35].

Although Taylor's law described well the overall dynamics of gut microbiota, some specific OTUs clearly deviated from the general trend (Fig. 4). To determine whether their behavior reflected specific ecological perturbations, we identified all OTUs that exhibited significant and abrupt increases in abundance during previously documented periods of travel in human A and enteric infection in human B[7] (Methods). Interestingly, these travel and infection-related OTUs corresponded to the outliers from Taylor's law (Fig. 4a,b, blue circles), showing on average ~10-fold greater variance than expected based on the Taylor's law trend (Supplementary Fig. 6a,c, Supplementary Table 1). Many of these OTUs were members of the Proteobacteria (OTU 13, family: Enterobacteriaceae, OTU 29, family: Pasteurellaceae, OTU 5771, family: Enterobacteriaceae in human A; OTU 13, family: Enterobacteriaceae in human B), which were associated with the microbiota perturbations[7] (Supplementary Table 1). Moreover, other OTUs, primarily belonging to the Firmicutes, that exhibited abrupt changes in abundances (OTU 25, family: Peptostreptococcaceae in human A; OTU 95, family: Ruminococcaceae, OTU 110, family Ruminococcaceae in human B) also displayed higher than expected temporal variability (Fig. 4a,b, purple circles, Supplementary Fig. 6c, Supplementary Table 1). These results suggest that macroecological relationships can be used to identify and characterize specific microbial taxa that are likely involved in periods of dysbiosis and other context-specific environmental perturbations.
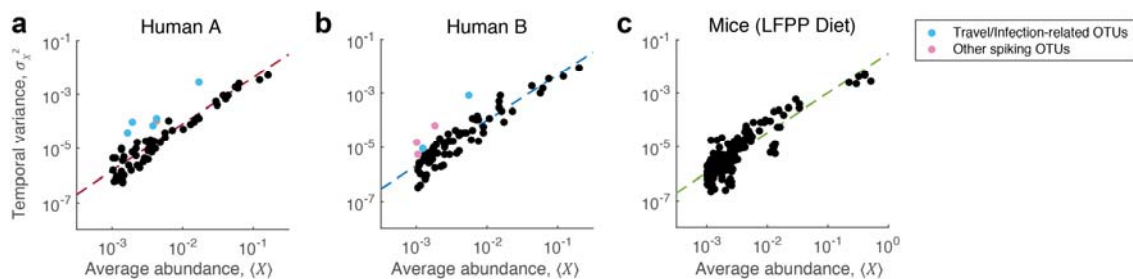

Fig. 4 | Taylor's power law in the gut microbiome. Mean and temporal variance of OTU abundances follow Taylor's power law of the form $\sigma_X^2 \propto \langle X \rangle^\beta$, with β =1.66±0.09, 1.60±0.08, 1.49±0.02 for humans A, B and LFPP mice respectively (mean ± s.d., see Methods). Each point corresponds to the average abundance and temporal variance of a single bacterial OTU. **a,b,** OTUs that exhibited temporary and abrupt increases in abundance are indicated as colored circles (Methods). Light blue circles indicate OTUs that exhibited significant increases in abundance specifically during periods of travel (human A) and enteric infection (human B). **c,** Data from each mouse on the LFPP diet are overlaid. Dashed lines indicate least-squares regression fits.

It is well established that the dynamics of diverse ecosystems are strongly affected by their environment[36]. Host dietary intake is a major environmental factor influencing gut bacterial abundances[8,17,37] and disease phenotypes[38,39]. Therefore, we next explored the effects of diet on the observed macroecological relationships describing gut microbiota dynamics. To that end, we used data from the study of Carmody et al.[8], who investigated fecal bacterial abundances in individually-housed mice fed either a low-fat, plant polysaccharide-based (LFPP) diet, or a high-fat, high-sugar (HFHS) diet. Our analysis revealed that the short-term dynamics of gut microbiota were significantly affected by the diets. While daily growth variability declined rapidly with increasing abundance in the LFPP mice (Fig. 5a, green), it remained more homogeneous across OTU abundances in the HFHS mice (Fig. 5a, purple, regression slopes $r = -0.17 \pm 0.03$ for the LFPP diet, -0.08 ± 0.02 for the HFHS diet, Z-test of regression coefficients p= 2.0e-5). The short-term behavior of gut microbiota in the LFPP mice reflects more pronounced diversity of bacterial

dynamics across OTU abundances. This diversity is partially lost on the HFHS diet, likely due to its significantly reduced nutrient complexity.

In addition to short-term fluctuations, we also investigated how different diets affected the long-term drift of gut microbiota. Interestingly, Hurst exponents were significantly larger in the HFHS mice, indicating substantially faster drift of bacterial abundances on this diet (Fig. 5b, Supplementary Fig. 3b, $H = 0.19 \pm 0.02$ for the HFHS diet, 0.08 ± 0.02 for the LFPP diet, Z-test p<1e-10). Previous studies have demonstrated diet-induced compositional shifts of gut microbiota[8,17,37] and a reduced gut bacterial diversity in Western populations attributed in part to altered dietary habits[40–42]. Our analysis shows that different diets not only affect the composition, but also significantly change the long-term dynamics of gut microbiota. In addition, we found that while the abundance drift of the Bacteroidetes and Firmicutes, the two major phyla in the mouse gut, were relatively similar on the HFHS diet ($H = 0.18 \pm 0.1$ for Bacteroidetes, $H = 0.18 \pm 0.03$ for Firmicutes), the Bacteroidetes exhibited significantly reduced drift on the LFPP diet as compared to the Firmicutes ($H = 0.03 \pm 0.06$, $H = 0.09 \pm 0.02$, Z-test p=3e-8). This suggests that while the LFPP diet decreased the long-term abundance drift of all taxa, the stability of the Bacteroidetes is particularly affected on this diet (see below).

Different diets may not only change overall gut microbiota dynamics, but also alter the temporal variability of individual taxa relative to the rest of the community. To understand taxa-specific changes, we examined Taylor's law in mice on the LFPP and HFHS diets (Fig. 5c,d). This analysis showed that power law exponents were significantly different between the two diets ($\beta = 1.49 \pm 0.02$ for the LFPP diet, $\beta = 1.86 \pm 0.07$ for the HFHS diet, Z-test p=1.5e-6). Interestingly, the temporal fluctuations of the Bacteroidetes (Fig. 5c,d, blue circles) exhibited significantly lower variability given their abundances on the LFPP diet, but not on the HFHS diet (hypergeometric test, p=2.4e-4, Supplementary Table 2, Methods). Notably, Bacteroidetes are known to metabolize a wide range of dietary fibers present in the LFPP diet[43,44] and are significantly lost during multigenerational propagation of mice on a low-fiber diet[41]. This suggests that specific members of the Bacteroidetes (OTU 118, OTU 237, OTU 364, family: Porphyromonadaceae, Supplementary Table 2) may exhibit both lower temporal variability and abundance drift by directly exploiting stable niches that are present on the LFPP diet and likely lost on the HFHS diet. Our results also demonstrate that macroecological analyses may be used to identify specific taxa whose temporal dynamics are altered between different diets.
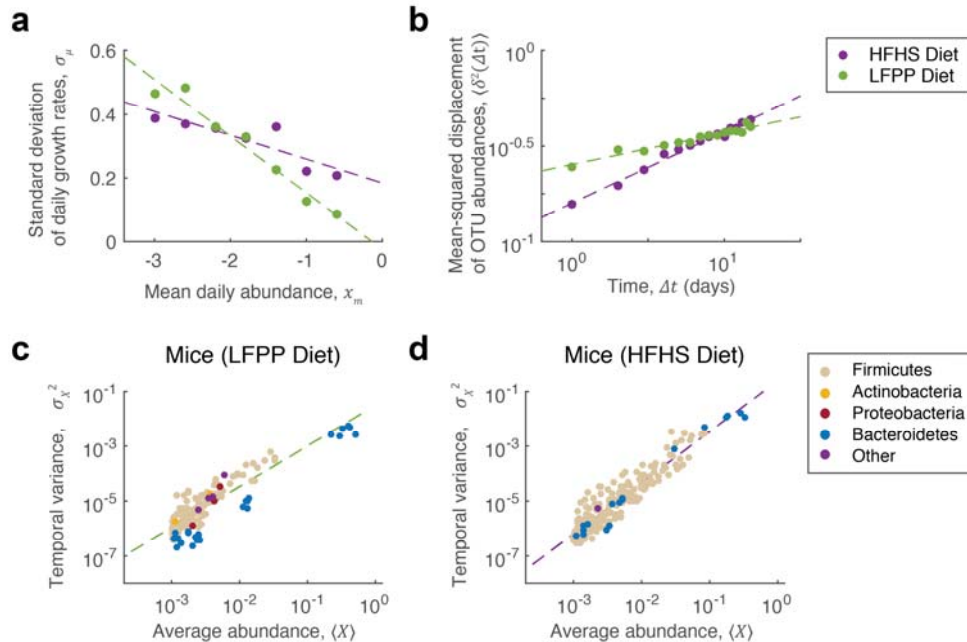
Fig. 5 | Dynamics of gut microbiota in mice fed different diets. a, OTUs in mice fed a low-fat plant-polysaccharide-based (LFPP) diet show a stronger dependence of daily growth rate variability (σ_μ) on mean daily abundance (x_m) compared to those fed a high-fat high-sugar (HFHS) diet (regression slopes $r = -0.17 \pm 0.03, r = -0.08 \pm 0.02$; mean$\pm$ s.d., LFPP and HFHS mice respectively). Data are aggregated across the three mice on each diet with dashed lines indicating least-squares regression fits. **b,** OTU abundances in the LFPP mice exhibit reduced long-term abundance drift compared to those in the HFHS mice ($H = 0.08 \pm 0.02, H = 0.19 \pm 0.02$). **c,d,** Taylor's law analysis shows differences in overall scaling of average OTU abundance versus temporal variance on each diet ($\beta = 1.49 \pm 0.02, \beta = 1.86 \pm 0.07$), driven by the temporal behavior of the Bacteroidetes in the LFPP mice (blue circles). Plots correspond to data combined from the three mice on each diet. Dashed lines indicate least-squares regression performed on the combined data.

Despite vastly different length and interaction scales, our study reveals that global dynamical patterns in the gut microbiome are strikingly similar to those observed in other highly diverse ecosystems. This similarity suggests that the temporal processes in both macroscopic and microbial communities are likely to be governed by a universal set of underlying mechanisms and principles. Thus, we envision that the quantitative statistical framework developed in macroecology[4,5,9,28] will also be important for analyzing gut microbiota dynamics. Moreover, the ability to easily perturb the composition and environment of gut bacteria, as well as monitor their abundances at high temporal resolution, creates an exciting opportunity to use the gut microbiome as a model system to explore general ecological relationships. We also anticipate that a quantitative ecological framework will be useful for understanding how host-specific and environmental factors influence the dynamics of gut microbiota. Our results suggest that the observed macroecological relationships can be used to identify both global dynamical changes and also specific taxa whose abnormal temporal behavior may serve as biomarkers for periods of illness and other ecological perturbations. Therefore, to further understand the role of the gut microbiome in human health, it will be important to investigate how quantitative macroecological relationships describing microbiota dynamics vary across large and densely-sampled human cohorts.

Methods

16S rRNA Sequence Analysis. Raw 16S rRNA sequencing data for humans A and B was obtained from the European Nucleotide Archive (accession number: PRJEB6518[7]). Raw sequencing data from humans M3, F4 and mice was obtained from the MG-RAST database[45] (4457768.3-4459735.3 for humans; 4597621.3-4599933.3 for mice). Sequences were analyzed with USEARCH 8.1[46] using an open clustering approach. For studies including unfiltered sequencing reads, filtering was performed using the –fastq_filter command with expected errors of 2. All reads were then truncated to 100bp, with shorter reads discarded. Following a conventional approach, reads were de-replicated and clustered at 97% sequence similarity using the –cluster_otus command to generate OTUs with a minimum of 2 sequences. Sequences were then assigned to OTUs using the –usearch_global command, resulting in OTU tables for each study. Taxonomic assignments were made to OTUs using the RDP classifier[47]. Sequencing reads from each sample were then rarefied to a depth of 25K, 17K and 25K for the two human studies (A/B, M3/F4) and one mouse study respectively using Qiime 1.8[48].

OTU Inclusion Criteria. To control for technical factors such as sample preparation and sequencing noise, analysis was restricted to OTUs passing two sets of criteria. First, OTUs were required to be present in over half of the samples within respective subjects. Second, OTUs were required to have a mean relative abundance > 1e-3 over the time series. The abundance cutoff corresponded to a mean of 25 (A, B, LFPP/HFHS mice) and 17 (M3 and F4) reads over respective sampling periods. The final analysis of human individuals included ~75 OTUs comprising ~90% of the reads assigned to an OTU in any given sample. For mice, these criteria resulted in the inclusion of ~70 OTUs in the HFHS diet and ~55 OTUs in the LFPP diet, comprising ~90% of reads assigned to an OTU in a given sample. Because the HFHS mice initially received a LFPP diet, the analysis of these mice began 5 days after the diet shift. For the calculation of residence and return times, different criteria were imposed (see below), as these analyses would be biased by a prevalence cutoff and were more robust to noise in OTU abundance levels.

Daily growth rates. Daily growth rates were defined as $\mu_k(t) = \log(X_k(t+1) / X_k(t))$, where $X_k(t)$ is the relative abundance of a given OTU k on day t. Distributions reflect community averages, with growth rates calculated for each OTU at all time points and aggregated over all OTUs. To estimate the variability of daily growth rate distributions within human subjects, each time series was divided into six consecutive time frames of equal length (estimates were insensitive to this number). Within each time frame, daily growth rates were calculated and maximum-likelihood estimation (MLE) was used to fit the Laplace distribution exponent, with the mean and standard deviation of these values reported in the main text. For the mouse study, standard deviations reflected variability across the three individual mice on each diet. Mean daily abundances x_m were defined as the mean of consecutive log OTU abundances, $x_m = \frac{1}{2}[\log(X(t+1)) + \log(X(t))]$. To estimate daily growth rate variability as a function of abundance, growth rates were binned by values of x_m using a bin size of 0.4 and standard deviations σ_μ were then calculated on the binned growth rates. For diet comparisons, growth rates were aggregated across the three mice on each diet. Growth rates and mean daily abundances were calculated using the base ten logarithm in all figures, with the natural log used for parameter estimation.

Hurst exponents. The mean-squared-displacement (MSD) of log OTU abundances was estimated as:

$$\langle \delta^2(\Delta t) \rangle = \frac{1}{N(T - \Delta t)} \sum_k \sum_i [\, x_k(t_i + \Delta t) - x_k(t_i) \,]^2$$

where the angled brackets denote a community average (over time and OTUs). Here, $x_k(t_i + \Delta t)$ is the log relative abundance of OTU k at time t_i, N is the total number of OTUs and T is the total length of the time series. A maximum time lag of 100 and 15 days were chosen for human and mice subjects respectively due to the finite length of each time series. Hurst exponents were then calculated by regressing $\langle \delta^2(\Delta t) \rangle$ against Δt on log-transformed axes. To estimate the variability of Hurst exponents within human subjects, time series were divided into six equal-length time frames as was done for growth rate calculations. Hurst exponents for individual OTUs were estimated in a similar fashion but with displacements restricted to time averages. For diet comparisons, Hurst exponents were additionally averaged over mice within each diet:

$$\langle \delta^2(\Delta t) \rangle_{diet} = \frac{1}{L} \sum_l \frac{1}{N_l(T_l - \Delta t)} \sum_k \sum_i [\, x_{l,k}(t_i + \Delta t) - x_{l,k}(t_i) \,]^2$$

where the outermost summation is over individual mice (L =3) on each diet.

Residence and return times. Residence times ($t_{res,k}$) of an OTU k corresponded to the number of consecutive time points between its appearance ($T_{a,k}$) and disappearance ($T_{d,k}$) in the community ($t_{res,k} = T_{d,k} - T_{a,k}$). Here, $T_{a,k}$ is any time point at which the OTU was detected at a finite read count with no reads detected on the previous collection date, and $T_{d,k}$ is the next time point at which reads were no longer detected. Return times t_{ret} were similarly defined as the number of consecutive time points between local disappearance ($T_{d,k}$) and reappearance ($T_{a,k}$) in the community ($t_{ret,k} = T_{a,k} - T_{d,k}$). Only intervals that fell entirely within the time frame of the study were included. A series of alternative criteria were also considered to ensure robustness of distributions. 1) To ensure results were not biased by detection sensitivity of sequencing, distributions were calculated for data subsampled to various sequencing depths (down to 1,000 reads per sample). 2) To account for false negatives in read detections, single read counts of zero interrupting a run of consecutive nonzero abundances were neglected. That is, an OTU with zero reads at time t was considered to be present in the community if that OTU was also present at times $t - 1$ and $t + 1$. 3) To control for false positives, single read abundances were neglected and treated as a zero count. Results were qualitatively insensitive to both sampling depth and the alternative read detection criteria. To estimate variability of distribution parameters within human individuals, OTUs were randomized into six equal-sized groups. Residence and return times were calculated within each group and exponents were then fitted using MLE, with means and standard deviations reported in the main text. Within diets, means and standard deviations were calculated across individual mice.

Taylor's power law. The mean abundance $\langle X_k \rangle$ and variance $\sigma^2_{X_k}$ for each OTU k was calculated over the time series. Taylor's exponents were obtained by performing linear regression of the log-transformed mean and variance across OTUs in each subject. To estimate variability of exponents within subjects, time series were divided into six consecutive time frames as described before. Spiking OTUs were defined as those whose abundance on any single day was greater than the average abundance over all other days by over 25-fold. Travel-related and infection-related OTUs in humans A and B were identified as those whose abundances spiked over 25-fold during the documented time periods[7]. For mice, Taylor's law outliers were identified using a likelihood-based approach. Briefly, linear regression on the log-transformed means and variances were performed on all but a single OTU k. The probability of observing the left out OTU k was assigned using a Gaussian likelihood function based on estimated residuals. All OTUs with probability less than $\alpha = 0.025$ were taken to be outliers. For diet comparisons, means and variances were aggregated across individual mice within diets groups.

Statistics. All statistical analysis was performed using custom scripts written in MATLAB (https://www.mathworks.com). Comparisons of various exponents between mouse diet groups were

performed by first calculating the relevant coefficient and associated standard error of combined data across the three mice in each diet group. Z-tests were then performed comparing the two coefficients associated with each diet group assuming normality of standard errors. Reported p-values refer to one-sided tests.

Data availability. All sequencing data used in this study can be downloaded from the ENA (https://www.ebi.ac.uk/ena/data/view/PRJEB6518 for humans A and B) and MG-RAST databases (https://www.mg-rast.org/linkin.cgi?project=mgp93 for humans M3 and F4; https://www.mg-rast.org/linkin.cgi?project=mgp11172 for mice). These data were used to generate all figures in the main text and supplement with the exception of Supplementary Figure 2.

Code availability. All MATLAB scripts used to perform data analysis and generate figures will be available on GitHub at the time of publication.

References

1. Costello, E. K., Stagaman, K., Dethlefsen, L., Bohannan, B. J. M. & Relman, D. a. The Application of Ecological Theory Toward An Understanding of the Human Microbiome. *Science (80-.).* **336,** 1255–1262 (2012).
2. Caporaso, J. G. *et al.* Global patterns of 16S rRNA diversity at a depth of millions of sequences per sample. *PNAS* **108,** 4516–4522 (2011).
3. Gohl, D. M. *et al.* Systematic improvement of amplicon marker gene methods for increased accuracy in microbiome studies. *Nat. Biotechnol.* **34,** 942–949 (2016).
4. Marquet, P. a *et al.* Scaling and power-laws in ecological systems. *J. Exp. Biol.* **208,** 1749–1769 (2005).
5. Azaele, S., Volkov, I. & Maritan, A. Statistical mechanics of ecological systems: Neutral theory and beyond. *Rev. Mod. Phys.* **88,** 1–31 (2016).
6. Caporaso, J. G. *et al.* Moving pictures of the human microbiome. *Genome Biol.* **12,** R50 (2011).
7. David, L. A. *et al.* Host lifestyle affects human microbiota on daily timescales. *Genome Biol.* **15,** R89 (2014).
8. Carmody, R. N. *et al.* Diet dominates host genotype in shaping the murine gut microbiota. *Cell Host Microbe* **17,** 72–84 (2015).
9. Keitt, T. H. & Stanley, H. E. Dynamics of North American breeding bird populations. *Nature* **393,** 257–260 (1998).
10. Keitt, T. H., Amaral, L. A. N., Buldyrev, S. V & Stanley, H. E. Scaling in the growth of geographically subdivided populations: invariant patterns from a continent-wide biological survey. *Philos. Trans. R. Soc. London* **357,** 627–633 (2002).
11. Sun, J., Cornelius, S. P., Janssen, J., Gray, K. A. & Motter, A. E. Regularity underlies erratic population abundances in marine ecosystems. *Philos. Trans. R. Soc. B* **12,** 1–7 (2015).
12. Azaele, S., Pigolotti, S., Banavar, J. R. & Maritan, a. Dynamical evolution of ecosystems. *Nature* **444,** 926–928 (2006).
13. Stanley, M. H. R. *et al.* Scaling behaviour in the growth of companies. *Nature* **379,** 804–806 (1996).
14. Faust, K., Lahti, L., Gonze, D., de Vos, W. M. & Raes, J. Metagenomics meets time series analysis: Unraveling microbial community dynamics. *Curr. Opin. Microbiol.* **25,** 56–66 (2015).
15. Faith, J. J. *et al.* The long-term stability of the human gut microbiota. *Science (80-.).* **341,** 1237439 (2013).
16. Dethlefsen, L. & Relman, D. A. Incomplete recovery and individualized responses of the human distal gut microbiota to repeated antibiotic perturbation. *PNAS* **108,** 4554–4561 (2011).
17. David, L. A. *et al.* Diet rapidly and reproducibly alters the human gut microbiome. *Nature* **505,** 559–63 (2014).
18. Smits, S. A. *et al.* Seasonal cycling in the gut microbiome of the Hadza hunter-gatherers of

Tanzania. *Science (80-.).* **357,** 802–806 (2017).

19. Shoemaker, W. R., Locey, K. J. & Lennon, J. T. A macroecological theory of microbial biodiversity. *Nat. Ecol. Evol.* **1,** 1–6 (2017).

20. Li, L. & Ma, Z. S. Testing the Neutral Theory of Biodiversity with Human Microbiome Datasets. *Sci. Rep.* **6,** 1–10 (2016).

21. Mitzenmacher, M. A Brief History of Generative Models for Power Law and Lognormal Distributions. *Internet Math.* **1,** 226–251 (2003).

22. Plerou, V., Amaral, L. a N., Gopikrishnan, P., Meyer, M. & Stanley, H. E. Similarities between the growth dynamics of university research and of competitive economic activities. *Nature* **400,** 433–437 (1999).

23. Niwa, H. S. Random-walk dynamics of exploited fish populations. *ICES J. Mar. Sci.* **64,** 496–502 (2007).

24. Hekstra, D. R. & Leibler, S. Contingency and statistical laws in replicate microbial closed ecosystems. *Cell* **149,** 1164–1173 (2012).

25. Metzler, R., Jeon, J., Cherstvy, G., Barkai, E. & Metzler, R. Anomalous diffusion models and their properties: non-stationarity, non-ergodicity, and ageing at the centenary of single particle tracking. *Phys. Chem. Chem. Phys.* **16,** 24128–24164 (2014).

26. Coyte, K. Z., Schluter, J. & Foster, K. R. The ecology of the microbiome: Networks, competition, and stability. *Science (80-.).* **350,** 663–666 (2015).

27. Gibbons, S. M., Kearney, S. M., Smillie, C. S. & Alm, E. J. Two dynamic regimes in the human gut microbiome. *PLoS Comput. Biol.* **13,** 1–20 (2017).

28. Suweis, S. *et al.* On species persistence-time distributions. *J. Theor. Biol.* **303,** 15–24 (2012).

29. Bertuzzo, E. *et al.* Spatial effects on species persistence and implications for biodiversity. *PNAS* **108,** 4346–4351 (2011).

30. Taylor, L. R. Aggregation, Variance and the Mean. *Nature* **189,** 732–735 (1961).

31. Taylor, L. R., Woiwod, I. P. & Perry, J. N. The Density-Dependence of Spatial Behaviour and the Rarity of Randomness. *J. Anim. Ecol.* **47,** 383–406 (1978).

32. Taylor, L. R. & Woiwod, I. P. Temporal Stability as a Density-Dependent Species Characteristic. *J. Anim. Ecol.* **49,** 209–224 (1980).

33. Anderson, R. M., Gordon, D. M., Crawley, M. J. & Hassell, M. P. Variability in the abundance of animal and plant species. *Nature* **296,** 245–248 (1982).

34. Kilpatrick, A. M. & Ives, A. R. Species interactions can explain Taylor's power law for ecological time series. *Nature* **19,** 65–68 (2003).

35. Ma, Z. Power law analysis of the human microbiome. *Mol. Ecol.* **24,** 5428–5445 (2015).

36. Brose, U., Hillebrand, H. & Brose, U. Biodiversity and ecosystem functioning in dynamic landscapes. *Philos. Trans. R. Soc. B* **371,** 1–8 (2016).

37. Wu, G. D. *et al.* Linking long-term dietary patterns with gut microbial enterotypes. *Science (80-.).* **334,** 105–108 (2011).

38. Turnbaugh, P. J. *et al.* An obesity-associated gut microbiome with increased capacity for energy harvest. *Nature* **444,** 1027–31 (2006).

39. Devkota, S. *et al.* Dietary-fat-induced taurocholic acid promotes pathobiont expansion and colitis in Il10−/− mice. *Nature* **487,** 104–108 (2012).

40. Yatsunenko, T. *et al.* Human gut microbiome viewed across age and geography. *Nature* **486,** 222–227 (2012).

41. Sonnenburg, E. D. *et al.* Diet-induced extinctions in the gut microbiota compound over generations. *Nature* **529,** 212–215 (2016).

42. Sonnenburg, E. D. & Sonnenburg, J. L. Starving our microbial self: The deleterious consequences of a diet deficient in microbiota-accessible carbohydrates. *Cell Metab.* **20,** 779–786 (2014).

43. Sonnenburg, E. D. *et al.* Specificity of polysaccharide use in intestinal bacteroides species determines diet-induced microbiota alterations. *Cell* **141,** 1241–1252 (2010).

44. Martens, E. C., Koropatkin, N. M., Smith, T. J. & Gordon, J. I. Complex glycan catabolism by the human gut microbiota: The bacteroidetes sus-like paradigm. *J. Biol. Chem.* **284,** 24673–24677 (2009).

45. Meyer, F. *et al.* The Metagenomics RAST Server: A Public Resource for the Automatic

Phylogenetic and Functional Analysis of Metagenomes. *BMC Bioinformatics* **9,** 1–8 (2008).

46.   Edgar, R. C. Search and clustering orders of magnitude faster than BLAST. 1–3 (2010).

47.   Wang, Q., Garrity, G. M., Tiedje, J. M., Cole, J. R. & Al, W. E. T. Naive Bayesian Classifier for Rapid Assignment of rRNA Sequences into the New Bacterial Taxonomy. **73,** 5261–5267 (2007).

48.   Caporaso, J. G. *et al.* QIIME allows analysis of high- throughput community sequencing data. *Nat. Methods* **7,** 335–336 (2010).

Author contributions

D.V. conceived the study. B.W.J. and R.U.S. performed all data analysis. P.D.D. contributed to data interpretation. All authors wrote the manuscript.

Competing interests

The authors declare no competing interests.

Materials and correspondence

Correspondence and requests for materials should be addressed to D.V.